# First-Principles Thermochemistry for the Combustion of a $TiCl_4$ and $AlCl_3$ Mixture

**Raphael Shirley, Yaoyao Liu, Tim S. Totton, Richard H. West, and Markus Kraft***

*Department of Chemical Engineering and Biotechnology, University of Cambridge, New Museums Site, Cambridge, United Kingdom*

*Received: June 4, 2009; Revised Manuscript Received: October 12, 2009*

$AlCl_3$ is added in small quantities to $TiCl_4$ fed to industrial reactors during the combustion synthesis of titanium dioxide nanoparticles in order to promote the rutile crystal phase. Despite the importance of this process, a detailed mechanism including $AlCl_3$ is still not available. This work presents the thermochemistry of many of the intermediates in the early stages of the mechanism, computed using quantum chemistry. The enthalpies of formation and thermochemical data for AlCl, AlO, AlOCl, $AlOCl_2$, $AlO_2$, $AlO_2Cl$, $AlOCl_3$, $AlO_2Cl_2$, $AlO_3ClTi$, $AlO_2Cl_2Ti$, $AlO_2Cl_4Ti$, $AlOCl_5Ti$, $AlO_2Cl_3Tia$ (isomer-a), $AlO_3Cl_2Ti$, $AlO_2Cl_5Ti$, $AlOCl_4Ti$, $AlO_2Cl_3Tib$ (isomer-b), $AlCl_7Ti$, $AlCl_6Ti$, $Al_2Cl_6$, $Al_2O_2Cl$, $Al_2O_2Cl_3$, $Al_2O_3Cl_2$, $Al_2O_2Cl_2$, $Al_2OCl_4$, $Al_2O_3$, and $Al_2OCl_3$ were calculated using density functional theory (DFT). A full comparison between a number of methods is made for one of the important species, AlOCl, to validate the use of DFT and gauge the magnitude of errors involved with this method. Finally, equilibrium calculations are performed to try to identify which intermediates are likely to be most prevalent in the high temperature industrial process and as a first attempt to characterize the nucleation process.

## Introduction

Titanium dioxide ($TiO_2$) is widely used as a pigment, as a catalyst support, and as a photocatalyst. The combustion of titanium tetrachloride ($TiCl_4$) to synthesize $TiO_2$ nanoparticles is a multimillion tonne per year industrial process.[1] In this "chloride" process, purified titanium tetrachloride is oxidized at high temperatures (1500−2000 K) in a pure oxygen plasma or flame to produce $TiO_2$ particles.[2,3] The overall stoichiometry of this oxidation process is

$$TiCl_{4(g)} + O_{2(g)} \rightarrow TiO_{2(\text{rutile nanoparticles})} + 2Cl_{2(g)} \quad (1)$$

$TiO_2$ crystallizes in three different forms: rutile, anatase, and brookite. $AlCl_3$ is often added to industrial reactors in order to promote formation of the rutile phase. The rutile phase is photochemically stable with a high refractive index compared to anatase and therefore preferred for pigmentary applications. $AlCl_3$ is added in small quantities (<5% mol), and it is unclear how significantly it alters the early gas phase reactions.

Although the chloride process is a mature technology, which has been used in industry since 1958, understanding of the gas-phase reactions of $TiCl_4$ remains incomplete.[4] Recently, West et al. have developed a detailed kinetic model for the process, including thermochemical data for the titanium oxychloride species involved.[5−7] However, these models do not attempt to include the impact of $AlCl_3$ on the reaction kinetics or on the properties of the particles formed. The paper by Akhtar et al. describes how $AlCl_3$ influences the crystal phase[8] of the particles but does not offer a mechanism to explain how. Some authors suggest that Al accelerates the anatase to rutile transformation,[9,10] but this is hard to reconcile with the theoretical studies showing that there is no significant thermodynamic bias between the doped phases.[11−13] It may be that Al lowers the barrier to phase transformation, but it is also possible that, in the industrial reactors, the phase is determined by the nucleation process. A small number of $TiAl_xCl_y$ species have been studied experimentally,[14,15] but the system with excess oxygen has not been investigated. Varga et al.[16] provide thermochemical data for some of the aluminum oxyhalides from computational studies but a number of possible species, particularly dimers, are missing. It is also possible that the impact of $AlCl_3$ is entirely physical in which case it would be useful to rule out any significant chemical interaction.

The aim of this work is to provide thermochemical data for important titanium/aluminum oxychloride species ($Al_iO_jCl_kTi_l$), which will enable the development of detailed kinetic models of the combustion of titanium tetrachloride with aluminum trichloride. The results from three DFT functionals are compared, giving some indication of the reliability of DFT for these transition metal oxychloride species.

Since the optical properties of $TiO_2$ depend strongly on particle size, a major technological issue in this large scale industrial process is precisely controlling the particle size distribution. The size distribution is expected to depend strongly on the particle nucleation rate, which in turn may depend strongly on the concentration of $AlCl_3$. We have used the new thermochemical data to perform equilibrium calculations to identify which intermediates are likely to be most prevalent in the high temperature industrial process. This is a first step toward understanding how $AlCl_3$ effects the nucleation process and how it determines crystal phase.

## Computational Method

**Species Generation.** As no reaction scheme currently exists for the gas phase reactions of $AlCl_3$, it was necessary to propose possible intermediate aluminum species that may by created by the reactions. These were then subject to geometry optimization calculations using density functional theory.

A script written in the Perl programming language was used to automatically generate possible aluminum species from those titanium species proposed by West et al.[7] in their mechanism

* Corresponding author. E-mail: mk306@cam.ac.uk.

10.1021/jp905244w CCC: $40.75 
Published on Web 11/04/2009

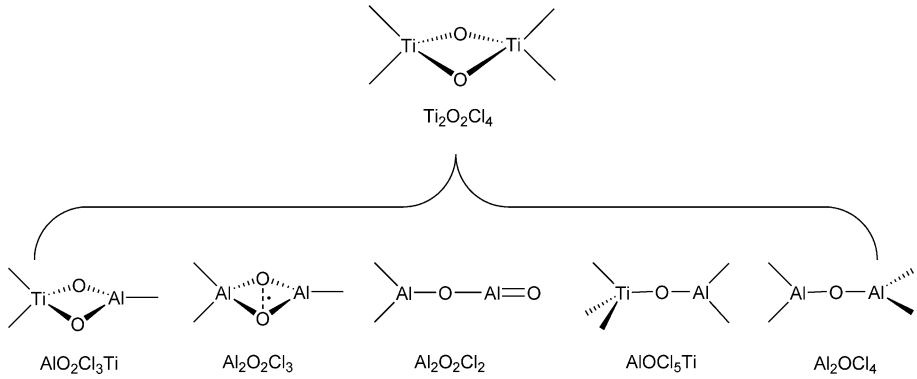


**Figure 1.** Generating possible aluminum-containing species from $Ti_2O_2Cl_4$. Unlabeled atoms are chlorine.

**TABLE 1: Calculated $\Delta_f H^\circ_{298.15K}$ Values (kJ/mol) for AlOCl from Different Ab Initio Methods and Basis Sets Using Eq 3[a]**

| | Hartree−Fock | | post-Hartree−Fock | | | | | DFT |
|---|---|---|---|---|---|---|---|---|
| basis set | HF | PUHF | MP2 | MP3 | MP4 | CCSD | CCSD(T) | B3LYP |
| 3-21G | −102 | −93 | −247 | −178 | −311 | −219 | −244 | −220 |
| 6-31G | −136 | −125 | −281 | −221 | −323 | −256 | −272 | −243 |
| 6-311G | −131 | −119 | −278 | −215 | −316 | −250 | −266 | −247 |
| 6-311G(d,p) | −81 | −68 | −194 | −147 | −212 | −175 | −191 | −203 |
| 6-311+G(d,p) | −96 | −82 | −210 | −139 | −232 | −189 | −204 | −216 |
| cc-pVDZ | −83 | −70 | −191 | −145 | −218 | −174 | −190 | −209 |
| cc-pVTZ | −109 | −94 | −229 | −181 | −247 | −204 | −221 | −234 |
| aug-cc-pVTZ | −112 | −97 | −239 | −190 | −256 | −211 | −229 | −236 |

[a] Calculations consist of single point energies based on the B97-1/6-311+G(d,p)-optimized geometry, with thermal contributions to enthalpy calculated from B97-1/6-311+G(d,p) frequencies.

for combustion synthesis of $TiO_2$. However, this is not as simple as a direct substitution of Al atoms for Ti atoms in each structure. There are two sources of additional complexity: (1) Some species have more than one Ti atom. Thus, aluminum-containing species may be generated with some or all Ti atoms substituted for Al atoms. (2) Valence differs between titanium (+4) and aluminum (+3) atoms. As such, species generated by direct substitution of Al for Ti are often unfeasible, and different aluminum-containing species may also be generated by removing one or more directly bonded atoms.

Thus, the Perl script uses conditional loops to systematically include possible permutations arising from (1) and (2) and exclude clearly unfeasible aluminum species (e.g., five directly bonded atoms). Figure 1 illustrates the possible aluminum-containing species generated (within reason) from $Ti_2O_2Cl_4$.

Where appropriate, further species were added heuristically in addition to those automatically generated. Many of the generated structures could not be made to converge to a stable geometry under DFT geometry optimization and are excluded.

**Quantum Chemistry Calculations.** For consistency and comparability with the previous work of West et al.[5] on $Ti_xO_yCl_z$ species, most calculations in this work were performed with the same three functionals: B3LYP,[17−19] B97-1,[20] and mPWPW91.[21,22] These were carried out using the Gaussian 03 package.[23]

Table 1 compares basis sets and ab initio methods for the single species AlOCl. The basis sets of Pople et al. (rows 1−5, Table 1) do not show systematic convergence of $\Delta_f H^\circ_{298.15K}$ with increasing basis set size. However, it is individual species' electronic energy that is directly affected by basis-set truncation error and Figure 2 shows inconsistent improvement in energies for each species used to calculate $\Delta_f H^\circ_{298.15K}$. Nonetheless, on average larger basis sets should yield better accuracy. The correlation-consistent basis sets do exhibit systematic improvement in the calculated formation enthalpies, which is expected by their design.

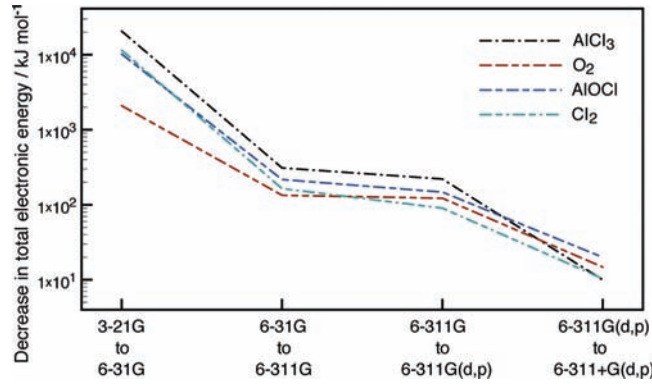


**Figure 2.** Decrease in total electronic energy with larger basis sets (i.e., reduction in basis-set truncation error). Energies are calculated by the B3LYP functional.

The accuracy of results from MP*n* methods, MP3 in particular, are erratic and possibly arise from sensitivity to spin contamination for the open-shell triplet ground state of $O_2$ (used to calculate $\Delta_f H^\circ_{298.15K}$, cf. eq 3).

The agreement between CCSD(T) and B3LYP for this geometry gives confidence to the DFT methods and reaction scheme employed in this work.

**Statistical Mechanics and Equilibrium Composition.** Heat capacities ($C_p^\circ$), thermal enthalpy ($H(T) - H(0\ K)$), and entropies ($S^\circ$) were calculated for temperatures in the range 100−4000 K using the rigid rotator harmonic oscillator (RRHO) approximation, taking unscaled vibrational frequencies and rotational constants from the B3LYP calculations. The contribution of the excited electronic states to the partition function is ignored.

Polynomials in the NASA[24] form were fitted to $C_p^\circ(T)/R$, $H^\circ$, and $S^\circ$ over the temperature ranges 100 − $x$ K and $x$ − 4000 K, constrained to ensure that all three functions are continuous and smooth across the boundary, $x$, which was varied to optimize

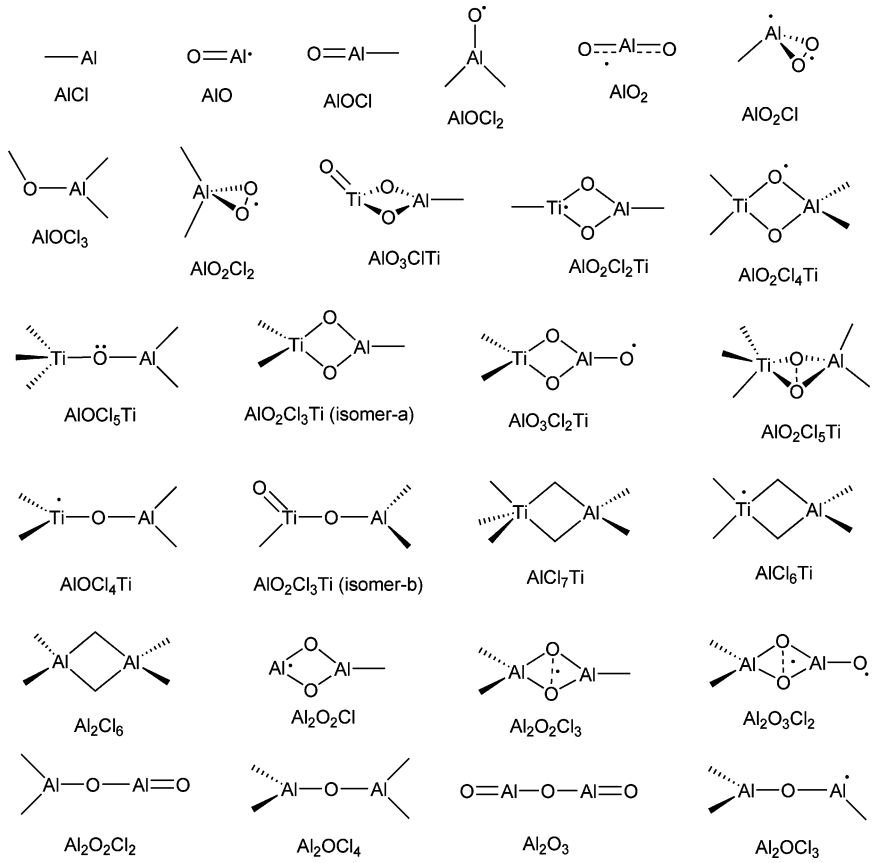


**Figure 3.** Molecular geometries after optimization with B3LYP/6-311+G(d,p). Unmarked atoms are chlorine. Exact geometries are available in the Supporting Information.

the fit. Using these NASA polynomials, the equilibrium composition as a function of temperature was calculated using the open source software Cantera.[25]

## Results and Discussion

**Geometries.** A large number of the species generated automatically and some of the species generated manually could not be made to converge to a sensible structure under geometry optimization with the B3LYP functional. Where a given molecule had numerous isomers, the lowest energy isomer was chosen and all others were neglected, except for the case of $AlO_2Cl_3Ti$, which had two isomers with very similar energies. Other species were omitted because they had very large enthalpies of formation and were only present to a negligible degree at equilibrium. Figure 3 shows the geometries of all the convergent species after optimization at the B3LYP/6-311+G(d,p) level of theory. The Gaussian output files and the geometries in mol format are available as Supporting Information.

**Enthalpy of Formation.** The paucity of literature thermochemical data for the aluminum oxychloride species investigated in this work meant it was not feasible to form isodesmic or isogyric reactions linking a species with unknown $\Delta_f H^\circ_{298.15K}$ to species for which $\Delta_f H^\circ_{298.15K}$ have been experimentally determined. An obvious starting point for AlCl, for instance, might have been the isogyric reaction (all three species are in singlet states)

$$\frac{1}{3}AlCl_3(g) + \frac{1}{3}Al_2O_3(g) \rightleftharpoons AlOCl(g) \qquad (2)$$

The NIST-JANAF thermochemical tables list $\Delta_f H^\circ_{298.15K} = -584.59$ kJ/mol for gaseous $AlCl_3$.[26] However, reliable thermochemical data for $Al_2O_3$ are only available for the *condensed* phase; the gaseous species has only been observed in plasmas.[27] Hence, eq 2 could not be used to determine $\Delta_f H^\circ_{298.15K}$ for AlOCl.

**TABLE 2: Literature Values of $\Delta_f H^\circ_{298.15K}$ (kJ/mol) for Some Aluminium Species Differ Significantly**

| $\Delta_f H^\circ_{298.15K}$ | CRC[28] | JANAF[26] |
|---|---|---|
| $Al_2O$ | −130.0 | −145.19 |
| AlO | 91.2 | 66.94 |
| AlCl | −47.7 | −51.46 |
| $AlCl_2$ | −331.0 | −280.33 |
| $AlCl_3$ | −583.2 | −584.59 |
| $TiCl_4$ | −763.2 | −763.16 |

The validity of the few available experimental data for $Al_xO_yCl_z$ species is also rather questionable. Varga et al.[16] suggest the JANAF value $\Delta_f H^\circ_{298.15K} = -348.11$ kJ/mol for $AlOCl_{(g)}$ may require review; they cite a value of −280.3 kJ/mol from experiment. Table 2 also shows the considerable discrepancy between values reported in JANAF and the CRC Handbook[28] for less observable aluminum species.

Given these constraints, the following reaction scheme was used to determine enthalpies of formation:

$$aAlCl_3(g) + bTiCl_4(g) + \frac{1}{2}cO_2(g) \rightleftharpoons Al_aO_cCl_dTi_b(g) + \frac{1}{2}(3a + 4b - d)Cl_2(g) \qquad (3)$$

This reaction is generally anisodesmic and often anisogyric; however, literature values of $\Delta_f H^\circ_{298.15K}$ for $AlCl_3$ and $TiCl_4$ are at least in good agreement with each other (Table 2). The main

**TABLE 3: Calculated $\Delta_f H^\circ_{298.15K}$ Values (kJ/mol) for Three Functionals with the 6-311+G(d,p) Basis Set Using Eq 3[a]**

| | DFT calculation | | | | literature | | |
|---|---|---|---|---|---|---|---|
| species | B3LYP | B97−1 | mPWPW91 | B3LYP[b] | JANAF[26] | CRC[28]/other | used |
| AlCl | −74 | −57 | −77 | −85 | −51 | −47.7 | −57 |
| AlO | 75 | 101 | 58 | 51 | 67 | 91.2 | 75 |
| AlOCl | −216 | −199 | −230 | −236 | −348 | −280.3[16] | −236 |
| AlOCl | −412 | −399 | −396 | −424 | | | −412 |
| AlO | −49 | | −72 | −79 | −86 | | −79 |
| AlOCl | −118 | −101 | −138 | −145 | | | −118 |
| $AlOCl_3$ | −514 | | | | | | −514 |
| $AlO_2Cl_2$ | −471 | −468 | −480 | −494 | | | −471 |
| $AlO_3ClTi$ | −957 | | | | | | −957 |
| $AlO_2Cl_2Ti$ | −936 | | | | | | −936 |
| $AlO_2Cl_4Ti$ | −1230 | | | | | | −1230 |
| $AlOCl_5Ti$ | −1107 | −1091 | −1058 | | | | −1107 |
| $AlO_2Cl_3Tia$ | −1229 | −1214 | −1223 | | | | −1214 |
| $AlO_3Cl_2Ti$ | −1044 | −1017 | −1021 | | | | −1017 |
| $AlO_2Cl_5Ti$ | −1291 | −1326 | | | | | −1326 |
| $AlOCl_4Ti$ | −1117 | | | | | | −1117 |
| $AlO_2Cl_3Tib$ | −1157 | | | | | | −1157 |
| $AlCl_7Ti$ | −1361 | | | | | | −1361 |
| $AlCl_6Ti$ | −1207 | | | | | | −1207 |
| $Al_2Cl_6$ | −1255 | −1274 | −1270 | | −1295 | | −1274 |
| $Al_2O_2Cl$ | −657 | | | | | | −657 |
| $Al_2O_2Cl_3$ | −1030 | −1012 | −1032 | | | | −1030 |
| $Al_2O_3Cl_2$ | −842 | | | | | | −842 |
| $Al_2O_2Cl_2$ | −815 | | | | | | −815 |
| $Al_2OCl_4$ | −1186 | | | | | | −1186 |
| $Al_2O_3$ | −441 | −397 | | | | | −441 |
| $Al_2OCl_3$ | −836 | | | | | | −836 |

[a] Calculations consist of geometry optimization and vibrational analysis with the specified functional. The final column indicates the values used for equilibrium calculations. [b] With the aug-cc-pVTZ basis set.

source of error in anisogyric reactions is due to systematic errors associated with given bonds where correlation energy is inaccurate at computationally affordable levels of theory.[29] However, these errors are in general likely to be smaller than or at least comparable to errors that might propagate through a series of coupled isodesmic/isogyric reactions with unreliable experimental $\Delta_f H^\circ_{298.15K}$ of the order of those seen in Table 2. If and when accurate experimental data become available, enthalpies can be rapidly recalculated from the information available in the Supporting Information.

Calculated formation enthalpies are consolidated in Table 3 alongside the few literature values that exist. The right-hand column shows the value that was used for the equilibrium calculations performed here. The enthalpy that is chosen for the equilibrium calculations is that calculated using B3LYP or, if experimental data is available, that theoretical value that is closest to the mean of the experimental values. The absence of reliable experimental data makes validation of the $\Delta_f H^\circ_{298.15K}$ values somewhat difficult. However, where available, the literature values agree reasonably well ($\pm\sim$ 40 kJ/mol). Agreement between the pure DFT (mPWPW91) and hybrid functionals (B3LYP, B97-1) is also good; these are calculated independently and thus their consistency gives confidence to the results. For example, the literature value of $\Delta_f H^\circ_{298.15K} = -1295$ kJ/mol for $Al_2Cl_6$[26] agrees well with −1255, −1270, and −1274 kJ/mol calculated by B3LYP, B97-1, and mPWPW91, respectively; the spread between functionals is 19 kJ/mol in this case. Errors of this order of magnitude are expected and consistent with those obtained by West et al.[5] for titanium oxychloride species. Equation 3 is still preferred over direct computation of $\Delta_f H^\circ_{298.15K}$ using atomization reactions; there is vastly more electronic correlation energy in molecules than in a collection of single atoms and retaining at least some bonds is always preferable *provided* the reference formation enthalpies taken from literature are reliable. West et al.[5] demonstrated a spread of 253 kJ/mol between formation enthalpies for $TiO_2Cl_3$ computer, with these functionals, through atomization (−865, −612, and −694 kJ/mol), which reduced to a spread of 38 kJ/mol when determined through an isogyric reaction.

**Thermochemistry.** Table 4 shows computed molecular and standard thermochemical data for species convergent under geometry optimization at the B3LYP/6-311+G(d,p) level of theory. Excited electron states are not considered. The smallest excitation energy was for $Al_2O_3Cl_2$ where the singlet state was found to be 130 kJ/mol higher than the triplet state and thus does not contribute significantly to the thermochemistry. This was also the only species to favor the higher spin state, which yields a $C_{2v}$ conformation and higher symmetry order than the $C_1$ singlet-state structure. In other species, the lowest-energy states of different spin state from the ground state were typically several hundred kJ/mol higher in energy, and thus contribution of these to the molecular partition function will be insignificant. It is instructive to compare the entropy to the sparse literature values in order to reassure ourselves that the equilibrium plots are meaningful. Entropy makes a comparable contribution to the free energy at high temperatures and at very high temperatures (>2000 K) dominates the free energy.

Table 5 shows that agreement for the entropy is stronger than for $\Delta_f H^\circ_{298.15K}$. This is probably because DFT produces reliable geometries and entropy is not directly affected by errors due to bond energies. It also goes some way to validating the RRHO assumption for this system and suggests that electronic contributions are not significant. Experimentally measured enthalpies of formation would be useful for improving thermochemistry. At the high temperatures of an industrial reactor enthalpy and entropy are of similar importance to the equilibrium concentration.

**Equilibrium Composition.** Computed equilibrium data are shown in Figure 4 for a mixture initially containing $AlCl_3$ and

**TABLE 4: Standard Thermochemistry at 298.15 K and Molecular Properties Calculated at the B3LYP/6-311+G(d,p) Level of Theory for Stable Electronic Ground States Using Eq 3[a]**

| species | $g$ | $\Delta_f H^\circ_{298.15K}$ (kJ/mol) | $S^\circ_{298.15\ K}$ (J/mol K) | rot. const. (GHz) | vibrational frequencies ($cm^{-1}$) |
|---|---|---|---|---|---|
| AlCl | 1 | −74 | 228 | 7.0380 | 452 |
| AlO | 2 | 75 | 219 | 18.5982 | 925 |
| AlOCl | 1 | −216 | 248 | 3.0948 | 178, 178, 485, 1108 |
| $AlOCl_2$ | 2 | −412 | 320 | 5.0340 2.1351 1.4992 | 143, 153, 213, 425, 624, 818 |
| $AlO_2$ | 2 | −49 | 236 | 5.7265 | 215, 215, 768, 826 |
| $AlO_2Cl$ | 3 | −118 | 313 | 14.388 2.5526 2.4810 | 143, 161, 411, 478, 605, 1144 |
| $AlOCl_3$ | 1 | −514 | 363 | 2.4067 1.1790 0.7913 | 77, 85, 137, 215, 218, 412, 609, 629, 906 |
| $AlO_2Cl_2$ | 2 | −471 | 340 | 2.8383 2.0287 1.2715 | 141, 155, 164, 198, 398, 461, 626, 675, 1135 |
| $AlO_3ClTi$ | 1 | −957 | 355 | 7.0330 0.8439 0.8017 | 78, 131, 181, 248, 312, 356, 559, 562, 707, 768, 847, 1038 |
| $AlO_2Cl_2Ti$ | 2 | −936 | 384 | 9.8416 0.5366 0.5088 | 29, 73, 115, 165, 257, 312, 420, 558, 578, 725, 767, 842 |
| $AlO_2Cl_4Ti$ | 2 | −1230 | 470 | 0.9708 0.4985 0.3581 | 34, 54, 84, 97, 108, 125, 170, 188, 276, 282, 399, 415, 448, 500, 554, 587, 685, 830 |
| $AlOCl_5Ti$ | 3 | −1107 | 534 | 0.7408 0.2748 0.2697 | 8, 28, 29, 60, 76, 97, 130, 141, 193, 243, 255, 284, 289, 369, 449, 585, 618, 996 |
| $AlO_2Cl_3Tia$ | 1 | −1157 | 464 | 1.4896 0.3705 0.3407 | 15, 28, 38, 71, 109, 153, 207, 259, 277, 332, 448, 591, 616, 994, 1071 |
| $AlO_3Cl_2Ti$ | 2 | −1044 | 401 | 1.7052 0.8143 0.6182 | 58, 106, 111, 164, 166, 177, 318, 332, 465, 505, 577, 683, 762, 768, 939 |
| $AlO_2Cl_5Ti$ | 1 | −1291 | 514 | 0.7465 0.3527 0.2843 | 27, 29, 56, 93, 101, 116, 129, 159, 185, 193, 241, 244, 280, 363, 382, 461, 471, 490, 601, 661, 755 |
| $AlOCl_4Ti$ | 2 | −1117 | 479 | 1.0230 0.3249 0.3177 | 10, 30, 32, 84, 95, 135, 148, 248, 257, 307, 404, 484, 587, 620, 994 |
| $AlO_2Cl_3Tib$ | 1 | −1229 | 406 | 1.7036 0.5327 0.4408 | 47, 97, 104, 148, 166, 174, 284, 326, 422, 504, 576, 590, 763, 767, 852 |
| $AlCl_7Ti$ | 1 | −1361 | 540 | 0.6225 0.2666 0.2536 | 13, 27, 74, 94, 101, 110, 123, 139, 160, 168, 168, 195, 216, 288, 335, 371, 433, 467, 492, 511, 596 |
| $AlCl_6Ti$ | 2 | −1207 | 503 | 0.7476 0.3465 0.2870 | 23, 48, 78, 83, 84, 106, 118, 154, 163, 194, 266, 291, 325, 376, 429, 491, 498, 602 |
| $Al_2Cl_6$ | 1 | −1255 | 473 | 0.7768 0.3902 0.3204 | 22, 63, 95, 116, 117, 129, 137, 165, 175, 217, 263, 311, 331, 412, 475, 514, 608, 617 |
| $Al_2O_2Cl$ | 2 | −657 | 322 | 9.7125 1.4497 1.2614 | 116, 151, 336, 352, 594, 628, 730, 762, 837 |
| $Al_2O_2Cl_3$ | 2 | −1030 | 416 | 1.8714 0.5182 0.4345 | 23, 110, 125, 139, 158, 201, 255, 280, 445, 446, 567, 586, 664, 714, 902 |
| $Al_2O_3Cl_2$ | 3 | −842 | 409 | 1.8678 0.7845 0.6072 | 27, 129, 130, 139, 173, 200, 263, 306, 437, 477, 588, 655, 694, 718, 972 |
| $Al_2O_2Cl_2$ | 1 | −815 | 384 | 2.2057 0.6983 0.5304 | 42, 71, 134, 174, 204, 287, 297, 349, 576, 620, 1000, 1209 |
| $Al_2OCl_4$ | 1 | −1186 | 445 | 1.1094 0.3538 0.3538 | 13, 39, 39, 110, 155, 179, 179, 280, 280, 323, 451, 612, 612, 669, 1113 |
| $Al_2O_3$ | 1 | −441 | 293 | 1.0077 | 71, 71, 186, 199, 312, 313, 420, 929, 1137, 1234 |
| $Al_2OCl_3$ | 2 | −836 | 425 | 1.8729 0.5101 0.4305 | 17, 47, 61, 134, 173, 237, 264, 362, 480, 605, 632, 1079 |

[a] The electronic degeneracy, $g$, is included.

$TiCl_4$ at conditions similar to those of the industrial chloride process[8] using thermochemical data calculated by this work. In industrial reactors it is common to use quantities of $AlCl_3$ ranging from 0 to 10% mol.[30] We first tested a number of low concentrations of $AlCl_3$ to gauge the sensitivity to initial concentration. In fact the behavior of the high concentration species is very *insensitive* to the amount of Al. We therefore chose a relatively large amount of $AlCl_3$ (5% mol) to produce instructive graphs that highlight the impact of Al. Figure 4 incorporates the titanium species from the $TiO_2$ mechanism proposed by West et al.[7] Thermochemical data for $TiCl_x$ ($x$ = 1, ..., 4), TiO, $TiO_2$, chlorine oxides and standard gases were taken from the NASA database.[31] Figure 5 is also included, which shows only the very upper part of the concentration plot in order to show the specific species that are most stable. Interestingly, $AlCl_3$ is the most stable aluminum species across the temperature range.

For clarity, the individual species concentrations in Figure 4 have been consolidated into the following groups: Ti oxychlorides (TiOCl, $TiOCl_2$, $TiOCl_3$, $TiO_2Cl_2$, $TiO_2Cl_3$, $Ti_2O_2Cl_3$, $Ti_2O_2Cl_4$, $Ti_2O_3Cl_2$, $Ti_2O_3Cl_3$, $Ti_3O_4Cl_4$, $Ti_5O_6Cl_8$, $Ti_2O_2Cl_6$, $Ti_2O_2Cl_5$, and $TiCl_2OCl$), Al chlorides ($Al_2Cl_6$, $AlCl_2$, $AlCl_3$, and AlCl), Ti chlorides ($TiCl_4$, $TiCl_3$, $TiCl_2$, and TiCl), chlorine oxides (ClO, $Cl_2O$, and $ClO_2$), Al monomers ($AlO_2Cl_2$, $AlOCl_2$, $AlO_2Cl$, AlOCl, $AlOCl_3$, $AlO_2$, and AlO), Ti−Al species ($AlO_3ClTi$, $AlO_2Cl_2Ti$, $AlO_2Cl_4Ti$, $AlO_3Cl_2Ti$, $AlO_2Cl_3Tia$, $AlO_2Cl_5Ti$, $AlOCl_5Ti$, $AlOCl_4Ti$, $AlO_2Cl_3Tib$, $AlCl_7Ti$, and $AlCl_6Ti$), and Al dimers ($Al_2O_3Cl_2$, $Al_2O_2Cl_3$, $Al_2O_2Cl_2$, $Al_2OCl_4$, $Al_2OCl_3$, $Al_2O_2Cl$, and $Al_2O_3$). There are ~50 species overall in the system. Oxygen and chlorine gases have been omitted from Figure 4, as their overall concentrations show little variation with temperature. The computed equilibrium compositions at other sensible initial $AlCl_3$ concentrations do not differ considerably with respect to the logarithmic scale, nor did pressure influence the position of equilibrium substantially.

$AlO_2Cl_2Ti$, $AlO_3ClTi$, and $AlOCl_4Ti$ are the most populous species containing both titanium and aluminum but none of these is present above a mole fraction of $10^{-5}$ at temperatures below 2000 K. This suggests that there is little interaction between $AlCl_3$ and $TiCl_4$ in the gas phase. Comparison to the equilibrium plots reported by West et al.[6] show that the new aluminum species have little to no effect on the equilibrium curves of the titanium species when $AlCl_3$ is present at the low concentrations used in industry. However, It is still possible that $AlCl_3$ reacts to form $Al_2O_3$ particles much faster than $TiCl_4$ decomposes and that these $Al_2O_3$ particles act as nucleation sites. Further investigation in to the gas phase kinetics is required.

**TABLE 5: Comparison of $S^{\circ}_{298.15K}$ Values (J/mol K) for Three Functionals with the 6-311+G(d,p) Basis Set[a]**

| | DFT calculation | | | | literature | | max. error | |
|---|---|---|---|---|---|---|---|---|
| species | B3LYP | B97-1 | mPWPW91 | B3LYP[b] | JANAF[26] | CRC[28]/other | DFT | lit. |
| $TiCl_4$ | 353.4 | 353.8 | 355.2 | | 354.8 | 353.2 | 1.8 | 2.0 |
| $Cl_2$ | 223.6 | 223.3 | 223.7 | 223.1 | 223.1 | 223.1 | 0.6 | 0.6 |
| $O_2$ | 205.1 | 205.1 | 205.3 | 205.0 | 205.1 | 205.2 | 0.2 | 0.2 |
| $AlCl_3$ | 313.9 | 313.9 | 314.9 | 314.0 | 314.4 | | 1.0 | 0.4 |
| AlCl | 228.3 | 228.2 | 228.4 | 228.3 | 228.0 | 228.1 | 0.2 | 0.4 |
| AlO | 218.7 | 218.7 | 218.7 | 218.6 | 218.3 | 218.4 | 0.1 | 0.4 |
| AlOCl | 247.7 | 247.7 | 248.4 | 247.7 | 248.9 | | 0.7 | 0.4 |
| $AlOCl_2$ | 319.7 | 319.9 | 322.5 | 319.3 | | | 3.2 | |
| $AlO_2$ | 236.3 | | 236.4 | 236.5 | 251.8 | | 0.3 | 15.3 |
| $AlO_2Cl$ | 313.2 | 312.9 | 314.1 | 312.8 | | | 1.3 | |
| $AlOCl_3$ | 362.7 | | | | | | | |
| $AlO_2Cl_2$ | 340.0 | 345.8 | 347.5 | 345.3 | | | 7.5 | |
| $AlO_3ClTi$ | 355.4 | | | | | | | |
| $AlO_2Cl_2Ti$ | 384.3 | | | | | | | |
| $AlO_2Cl_4Ti$ | 469.5 | | | | | | | |
| $AlOCl_5Ti$ | 533.6 | 532.3 | 538.9 | | | | 6.6 | |
| $AlO_2Cl_3Tia$ | 405.8 | 406.0 | 409.1 | | | | 3.2 | |
| $AlO_3Cl_2Ti$ | 401.0 | 401.4 | 406.0 | | | | 5.0 | |
| $AlO_2Cl_5Ti$ | 513.6 | 508.4 | | | | | 5.1 | |
| $AlOCl_4Ti$ | 478.6 | | | | | | | |
| $AlO_2Cl_3Tib$ | 463.6 | | | | | | | |
| $AlCl_7Ti$ | 539.9 | | | | | | | |
| $AlCl_6Ti$ | 503.2 | | | | | | | |
| $Al_2Cl_6$ | 473.2 | 473.7 | 476.7 | | 475.0 | | 3.5 | 1.8 |
| $Al_2O_2Cl$ | 322.1 | | | | | | | |
| $Al_2O_2Cl_3$ | 416.1 | 416.9 | 392.6 | | | | 24.2 | |
| $Al_2O_3Cl_2$ | 409.4 | | | | | | | |
| $Al_2O_2Cl_2$ | 384.2 | | | | | | | |
| $Al_2OCl_4$ | 444.9 | | | | | | | |
| $Al_2O_3$ | 293.3 | 298.9 | | | | | 5.6 | |
| $Al_2OCl_3$ | 425.1 | | | | | | | |

[a] All values computed from frequencies obtained after geometry optimization with specified functional. Final column indicates maximum unsigned error between DFT-DFT and DFT-literature values. [b] With the aug-cc-pVTZ basis set.

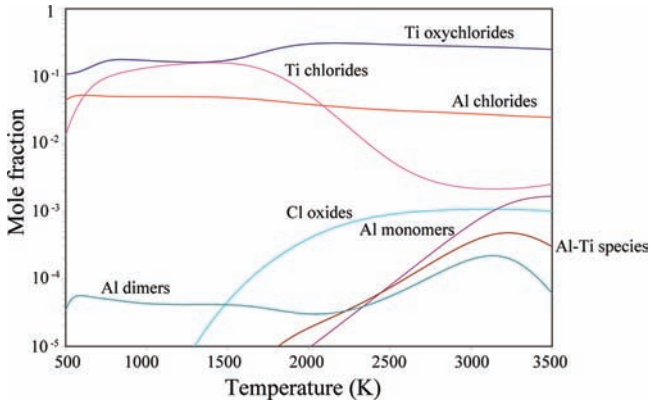


**Figure 4.** Computed equilibrium for a *combined* Al/Ti system, initially 5 mol % $AlCl_3$, 47.5 mol % $TiCl_4$ and $O_2$ at 101.3 kPa. Thermochemical data for Ti species from[7] and the NASA database.[31] For clarity, individual species are grouped, with oxygen/chlorine omitted.

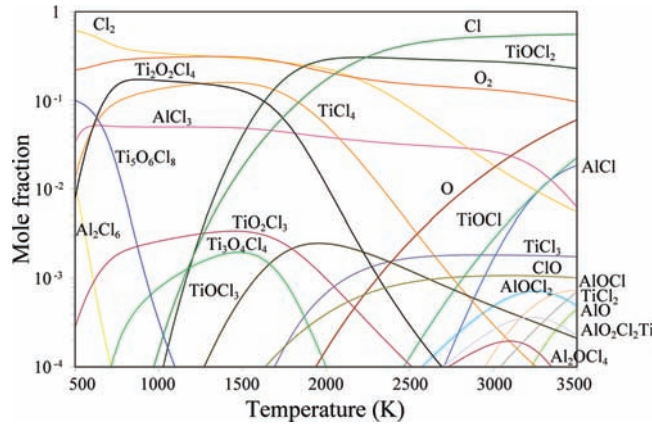


**Figure 5.** Computed equilibrium for a *combined* Al/Ti system, initially 5 mol % $AlCl_3$, 47.5 mol % $TiCl_4$ and $O_2$ at 101.3 kPa. Thermochemical data for Ti species from[7] and the NASA database.[31] Only the very top of the equilibrium plot is shown. The majority of species are excluded.

## Conclusion

This work has extended the detailed thermochemistry of the gas-phase titanium oxychloride species investigated by West et al.[5] to a similar system of aluminum-containing species. These were not previously included in their work but play an important role in the industrial combustion synthesis of rutile $TiO_2$. New aluminum species have been proposed through automated species generation and investigated using ab initio and DFT methods of computational quantum chemistry. This enabled detailed thermochemical data to be computed for the generated species, many of which have not been reported in the literature and are impossible to obtain with currently available experimental techniques.

Using the thermochemical data, temperature-dependent equilibrium compositions were obtained through simulations at industrially relevant operating conditions. The aluminum−titanium species are only found to exist at very low concentrations. This seems to suggest that there is not a significant interaction between the two systems in the early stages of the reaction. It suggests that $AlCl_3$ is likely to influence the particle processes rather than the gas phase chemical reactions or that its impact

is purely physical. Further studies into the kinetics of the $TiCl_4$/$AlCl_3$/$O_2$ system are required to make reliable conclusions about the stage at which $AlCl_3$ might determine phase.

**Acknowledgment.** The authors thank Tioxide Europe Limited (TEL) for the financial support of RAS and the EPSRC for help in the form of research hopping Grant Number EP/E01724X-1.

**Supporting Information Available:** Thermochemistry in the form of NASA polynomial coefficients for the species AlCl, AlO, AlOCl, $AlOCl_2$, $AlO_2$, $AlO_2Cl$, $AlOCl_3$, $AlO_2Cl_2$, $AlO_3ClTi$, $AlO_2Cl_2Ti$, $AlO_2Cl_4Ti$, $AlOCl_5Ti$, $AlO_2Cl_3Tia$, $AlO_2Cl_2Ti$, $AlO_2Cl_5Ti$, $AlOCl_4Ti$, $AlO_2Cl_3Tib$, $AlCl_7Ti$, $AlCl_6Ti$, $Al_2Cl_6$, $Al_2O_2Cl$, $Al_2O_2Cl_3$, $Al_2O_3Cl_2$, $Al_2O_2Cl_2$, $Al_2OCl_4$, $Al_2O_3$, and $Al_2OCl_3$ is provided in the Cantera format. The Gaussian output files and geometries in mol format for all these species are also supplied. This material is available free of charge via the Internet at http://pubs.acs.org.

## References and Notes

(1) Emsley, J. *Molecules at an Exhibition*; Oxford University Press: New York, 1999.

(2) Gonzalez, R. A.; Musick, C. D.; Tilton, J. N. Process for controlling agglomeration in the manufacture of $TiO_2$. U.S. Patent 5,508,015, 1996.

(3) Deberry, J. C.; Robinson, M.; Pomponi, M.; Beach, A. J.; Xiong, Y.; Akhtar, K. Controlled vapor phase oxidation of titanium tetrachloride to manufacture titanium dioxide. U.S. Patent 6,387,347, 2002.

(4) Karlemo, B.; Koukkari, P.; Paloniemi, J. *Plasma Chem. Plasma Process.* **1996**, *16*, 59–77.

(5) West, R. H.; Beran, G. J. O.; Green, W. H.; Kraft, M. *J. Phys. Chem. A* **2007**, *111*, 3560–3565.

(6) West, R. H.; Celnik, M. S.; Inderwildi, O. R.; Kraft, M.; Beran, G. J. O.; Green, W. H. *Ind. Eng. Chem. Res.* **2007**, *46*, 6147–6156.

(7) West, R. H.; Shirley, R. A.; Kraft, M.; Goldsmith, C. F.; Green, W. H. *Combust. Flame* **2009**, *156*, 1764–1770.

(8) Akhtar, M. K.; Pratsinis, S. E.; Mastrangelo, S. V. R. *J. Mater. Res.* **1994**, *9*, 1241–1249.

(9) Lee, J. E.; Oh, S.-M.; Park, D.-W. *Thin Solid Films* **2004**, *457*, 230–234 (The 16th Symposium on Plasma Science for Materials (SPSM-16)).

(10) Reidy, D.; Holmes, J.; Morris, M. *J. Eur. Ceram. Soc.* **2006**, *26*, 1527–1534.

(11) Shirley, R.; Inderwildi, O. R.; Kraft, M. Electronic and optical properties of aluminium-doped anatase and rutile $TiO_2$ from ab initio calculations. *Technical Report 71*, **2009**; c4e-Preprint Series (http://como.cheng.cam.ac.uk).

(12) Steveson, M.; Bredow, T.; Gerson, A. R. *Phys. Chem. Chem. Phys.* **2002**, *4*, 358–365.

(13) Islam, M. M.; Bredow, T.; Gerson, A. *Phys. Rev. B* **2007**, *76*, 045217.

(14) Soerlie, M.; Oeye, H. A. *Inorg. Chem.* **1978**, *17*, 2473–2484.

(15) Hildenbrand, D. L.; Lau, K. H.; Mastrangelo, S. V. R. *J. Phys. Chem.* **1991**, *95*, 3435–3437.

(16) Varga, Z.; Hargittai, M. *Struct. Chem.* **2008**, *19*, 595–602.

(17) Becke, A. D. *J. Chem. Phys.* **1993**, *98*, 5648–5651.

(18) Lee, C. T.; Yang, W. T.; Parr, R. G. *Phys. Rev. B* **1988**, *37*, 785–789.

(19) Stephens, P. J.; Devlin, F. J.; Chabalowski, C. F.; Frisch, M. J. *J. Phys. Chem.* **1994**, *98*, 11623–11627.

(20) Hamprecht, F. A.; Cohen, A. J.; Tozer, D. J.; Handy, N. C. *J. Chem. Phys.* **1998**, *109*, 6264–6271.

(21) Perdew, J. P. In *Electronic Structure of Solids*; Ziesche, P., Eschrig, H., Eds.; Akademie Verlag: Berlin, 1991; p 11.

(22) Adamo, C.; Barone, V. *J. Chem. Phys.* **1998**, *108*, 664–675.

(23) Frisch, M. J.; *Gaussian 03, Revision C.02*; Gaussian, Inc.: Wallingford, CT, 2004.

(24) Gordon, S.; McBride, B. J. Computer Program for Calculation of Complex Chemical Equilibrium Composition, Rocket Performance, Incident and Reflected Shocks and Chapman-Jouguet Detonations. *Technical Report NASA-SP-273*, **1976**.

(25) Goodwin, D. G. An open source, extensible software suite for CVD process simulation. *Chemical Vapor Deposition XVI and EUROCVD 14*; Pennington: New Jersey, 2003; pp 155−162.

(26) Chase, M. W., Jr. *J. Phys. Chem. Ref. Data* **1998**, Monograph 9, I-II.

(27) Desai, S. R.; Wu, H.; Rohlfing, C. M.; Wang, L.-S. *J. Chem. Phys.* **1997**, *106*, 1309–1317.

(28) Standard thermodynamic properties of chemical substances. In *CRC Handbook of Chemistry and Physics*, 87th ed.; Lide, D. R., Ed.; Taylor and Francis: Oxford, 2007; Vol. 5-4.

(29) Cramer, C. J. *Essentials of Computational Chemistry*; Wiley: New York, 2003.

(30) Santos, P. C. Production of Titanium Dioxide. U.S. Patent 3,505,091, 1970.

(31) McBride, B. J.; Zehe, M. J.; Gordon, S. NASA Glenn Coefficients for Calculating Thermodynamic Properties of Individual Species. *Technical Report TP-2002-211556*, **2002**.

JP905244W